

Optimizing Czerny–Turner Spectrographs: A Comparison between Analytic Theory and Ray Tracing

JOSEPH READER

National Bureau of Standards, Washington, D. C. 20234

(Received 13 March 1969)

The analytic theory of aberrations has been used to derive an expression for the magnitude of the coma width of the image in the meridional plane in a Czerny–Turner spectrograph with unequal mirror radii. The calculated properties of a 4-m spectrograph with equal radii and a recently constructed 3.34-m spectrograph with unequal radii are compared with the results obtained by tracing individual rays. The agreement is excellent, in contrast to the results of Chandler [J. Opt. Soc. Am. 58, 895 (1968)]. The lateral position of the grating for complete elimination of coma found experimentally with the 3.34-m instrument is in fair agreement with the theory. A correction to the $\sqrt{3}$ longitudinal grating position is given for a Czerny–Turner spectrograph which results in a flatter focal surface.

INDEX HEADINGS: Aberrations; Geometrical optics; Grating; Ray tracing; Spectrograph.

The design of plane-grating spectrographs has undergone considerable development since Czerny and Turner’s demonstration of the superiority of a two-mirror system over a one-mirror system.¹ In general, the design problem may be summarized by the question: Where should the grating be placed in a two-mirror spectrograph so that the aberrations in the final slit images will be minimized and so that the final focal surface will be as flat as possible? In the past, most workers have dealt with this problem by applying classical geometrical optics. More recently Chandler² used a high-speed computer to trace a number of rays through a 4-m focal-length system to determine the image quality, and by iteration determined the optimum lateral position of the grating. The optimum position found by Chandler was significantly different from the position calculated from the known analytical expressions.

At the time Chandler’s paper was published I was aligning a newly constructed 3.34-m Czerny–Turner spectrograph designed for minimum coma according to analytic theory, and I was stimulated to look into this reported difference between the analytic theory and ray tracing. In the present paper, the results of this investigation are given. The results disagree with those of Chandler. Some brief extensions of the theory will also be given, as well as the calculated characteristics of the 3.34-m Czerny–Turner spectrograph, now in use in our laboratory.

CALCULATIONS

Coma Width of Image

We present here a calculation of the image width in the meridional plane in a two-mirror plane-grating spectrograph with mirror radii R_1 and R_2 . This is an extension of the work of Shafer, Megill, and Droppleman.³ We first calculate the angular aberration in the

parallel beam generated by the collimating mirror. Following Shafer, Megill, and Droppleman, we start with Beutler’s⁴ light-path function for a spherical mirror reduced to two dimensions. To terms of order w^3/r^2 , the light-path function F for rays travelling from an object point at r to an image point at r' is

$$F = r + r' - w(\sin\alpha + \sin\alpha') + \frac{w^2}{2} \left[\left(\frac{\cos^2\alpha}{r} - \frac{\cos\alpha}{R_1} \right) + \left(\frac{\cos^2\alpha'}{r'} - \frac{\cos\alpha'}{R_1} \right) \right] + \frac{1}{2} w^3 \left[\frac{\sin\alpha}{r} \left(\frac{\cos^2\alpha}{r} - \frac{\cos\alpha}{R_1} \right) + \frac{\sin\alpha'}{r'} \left(\frac{\cos^2\alpha'}{r'} - \frac{\cos\alpha'}{R_1} \right) \right].$$

The symbols are explained in Fig. 1. If we express F in terms of w' , the perpendicular distance to the principal ray, according to $w = w'/\cos\alpha'$ and apply Fermat’s principle with $r' = \infty$ to indicate a plane wave after reflection, we have

$$\frac{\partial F}{\partial w'} (\text{for } r' = \infty) = -\frac{1}{\cos\alpha'} (\sin\alpha + \sin\alpha') + \frac{w'}{\cos^2\alpha'} \left[\frac{\cos^2\alpha}{r} - \frac{\cos\alpha}{R_1} - \frac{\cos\alpha'}{R_1} \right] + \frac{3w'^2}{2 \cos^3\alpha'} \left[\frac{\sin\alpha}{r} \left(\frac{\cos^2\alpha}{r} - \frac{\cos\alpha}{R_1} \right) \right] = 0.$$

The first term is made zero by letting $\alpha' = -\alpha$, which is just the usual law of reflection. The linear term in w' is made zero by letting $r = \frac{1}{2} R_1 \cos\alpha$, which is the well-known meridional focal distance for off-axis points. The quadratic term in w' contains no other parameters which may be varied and thus represents the residual two-dimensional aberration referred to as coma. Evaluating this for an aperture corresponding to the projected

¹ M. Czerny and A. F. Turner, Z. Physik 61, 792 (1930).
² G. Chandler, J. Opt. Soc. Am. 58, 895 (1968).
³ A. Shafer, L. Megill, and L. Droppleman, J. Opt. Soc. Am. 54, 879 (1964).

⁴ H. G. Beutler, J. Opt. Soc. Am. 35, 311 (1945).

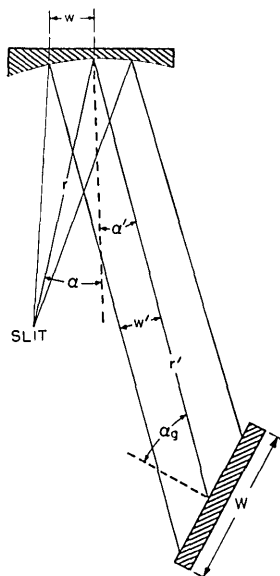


FIG. 1. Explanation of symbols for light-path function for spherical mirror in two dimensions.

grating width, we have

$$(\partial F / \partial w') \text{ (for } r' = \infty, \alpha' = -\alpha, r = \frac{1}{2}R_1 \cos \alpha, \\ w' = \frac{1}{2}W \cos \alpha_g) = \frac{3W^2 \cos^2 \alpha_g \sin \alpha}{4R_1^2 \cos^3 \alpha}.$$

This gives the angular aberration $\delta \alpha_g$ in the beam prior to diffraction by the grating. Differentiating the grating equation, $m\lambda = d(\sin \alpha_g + \sin \beta_g)$, we obtain the angular aberration after diffraction

$$\delta \beta_g = -\frac{\cos \alpha_g}{\cos \beta_g} \delta \alpha_g = -\frac{3W^2 \sin \alpha \cos^3 \alpha_g}{4R_1^2 \cos^3 \alpha \cos \beta_g}.$$

This corresponds to a transverse aberration in the focal plane of the camera mirror

$$\Delta_\alpha = \frac{1}{2}R_2 \cos \beta \delta \beta_g = -\frac{3W^2 R_2 \sin \alpha \cos \beta \cos^3 \alpha_g}{8R_1^2 \cos^3 \alpha \cos \beta_g},$$

where β is the off-axis angle at the camera mirror. This is the width of the image in the final focal field, due to the off-axis reflection at the collimating mirror. The coma generated by the off-axis reflection at the camera mirror is calculated by using Beutler's light-path function, with α , α' , and R_1 replaced by β , β' , and R_2 , respectively. We assume that the camera mirror is illuminated with a plane wave, so that $r = \infty$. The angular aberration in the reflected beam is then

$$(\partial F / \partial w') \text{ (for } r = \infty, \beta' = -\beta, r' = \frac{1}{2}R_2 \cos \beta, \\ w' = \frac{1}{2}W \cos \beta_g) = \frac{3W^2 \cos^2 \beta_g \sin \beta}{4R_2^2 \cos^3 \beta}.$$

This corresponds to a transverse aberration in the focal plane of the camera mirror

$$\Delta_\beta = \frac{1}{2}R_2 \cos \beta \frac{\partial F}{\partial w'} = \frac{3W^2 \cos \beta_g \sin \beta}{8R_2 \cos^2 \beta}.$$

The total coma width in the image is thus

$$\Delta = \Delta_\alpha + \Delta_\beta = \frac{3W^2 R_2 \cos^2 \alpha_g \cos \beta}{8 \cos^3 \alpha} \\ \times \left[\frac{\sin \beta \cos^2 \beta_g \cos^3 \alpha}{R_2^2 \cos^2 \alpha_g \cos^3 \beta} - \frac{\sin \alpha \cos \alpha_g}{R_1^2 \cos \beta_g} \right]. \quad (1)$$

The coma may be completely eliminated by arranging the optics so that

$$\frac{\sin \beta}{\sin \alpha} = \frac{R_2^2 \cos^3 \beta \cos^3 \alpha_g}{R_1^2 \cos^3 \alpha \cos^3 \beta_g}, \quad (2)$$

which is the coma-free condition given by Shafer, Megill, and Droppleman.³ A formula corresponding to Eq. (1) for the case of $R_1 = R_2$ as derived from the results of Rosendahl⁵ has been previously given in an unpublished Jarrell-Ash technical bulletin. When the off-axis angles are small, we may let $\cos^3 \beta \approx \cos^3 \alpha \approx 1$, $\sin \beta = \beta$, $\sin \alpha = \alpha$, and if $R_1 = R_2$ we obtain from Eq. (2) an approximate coma-free condition

$$\beta / \alpha = \cos^2 \alpha_g / \cos^2 \beta_g, \quad (3)$$

which is the relation for coma compensation given originally by Fastie.⁶

For a given spectrograph design and given angles of incidence and diffraction, the coma at the center or some other point of the plate can be eliminated by using the ratio $\sin \beta / \sin \alpha$ indicated in Eq. (2). As the grating rotates to different angles of incidence and diffraction, the coma can still be eliminated by translating the grating laterally so as to change α and β appropriately. For points on the plate that do not satisfy Eq. (2), the amount of coma present can be evaluated by Eq. (1).

There are a number of problems associated with a lateral translation of the grating, such as changes of focus, changes of the location of the entrance axis, and changes of the wavelength calibration of the grating table. For these reasons we note that, if possible, a lateral grating translation should be avoided.

The Super-Flat-Field Position

As shown experimentally by Fastie⁶ and theoretically by Khrshanovskii,⁷ a nearly flat focal field can be achieved by placing the grating at a distance $[1 - (1/\sqrt{3})]R_2$ from the camera mirror. This distance is measured along a line passing through the center of

⁵ G. Rosendahl, *J. Opt. Soc. Am.* **52**, 412 (1962).

⁶ W. G. Fastie, U. S. Patent 3,011,391 (1961).

⁷ S. A. Khrshanovskii, *Opt. Spectry.* (USSR) **9**, 207 (1960).

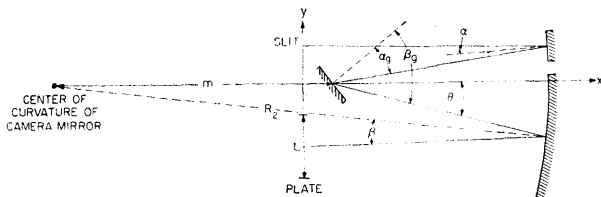


FIG. 2. Geometry of a Czerny-Turner spectrograph for plate-curvature considerations. The y axis is located at a distance $R_2/2$ from the center of curvature of the camera mirror.

curvature of the camera mirror and the center of the grating, as shown in Fig. 2. If this line is taken as the x axis, the results of both Khrshanovskii⁷ and Mielenz⁸ may be used to evaluate the shape of the focal surface in a Czerny-Turner spectrograph.

For an already assembled instrument, it may not be easy to determine the location of this x axis because the grating is usually inside the spectrograph and the center of curvature of the camera mirror is usually outside. However, if the camera mirror is large enough so that this imaginary line would intersect a point on the actual surface of the mirror, the x axis may be found by directing a narrow laser beam to the center of the grating, with the grating positioned so that the direct image falls on the camera mirror. (The location of the laser is not important as long as its beam hits the center of the grating.) If the grating is then rotated so that the direct image moves across the camera mirror toward the slit, the laser beam reflected from the camera mirror will return to the face of the grating. When the return beam coincides with the original beam, the laser beam between the grating and camera mirror coincides with the x axis. If the camera mirror is not large enough to make the original and return beams coincide, the desired distance can be evaluated from other measurable spectrograph dimensions, as given in the Appendix.

Mielenz⁸ has formulated the equation of the focal surface in terms of the angle θ , whose meaning for a Czerny-Turner spectrograph is given in Fig. 2. To an approximation that neglects terms of order θ^6 , the focal curve in the meridional plane is given by

$$\frac{x}{R_2} = -\frac{1}{4} \left[1 - 3 \left(\frac{m}{R_2} \right)^2 \right] \theta^2 + \frac{1}{48} \left[1 - 30 \left(\frac{m}{R_2} \right)^2 + 48 \left(\frac{m}{R_2} \right)^3 - 27 \left(\frac{m}{R_2} \right)^4 \right] \theta^4. \quad (4)$$

Setting the term in θ^2 equal to zero by placing the grating at the flat-field position, $m = R_2/\sqrt{3}$, yields a focal curve that deviates from the y -axis by a term proportional to θ^4 . In spectrographs that are either very fast or have an extensive plate, this θ^4 term may cause the focal curve to deviate significantly from a straight

line. Mielenz⁸ has shown that, for an Ebert-type spectrograph, a correction to the $m = R_2/\sqrt{3}$ position may be made to make the focal curve parallel to the y axis in the θ^4 approximation. This is done by setting $m = (R_2/\sqrt{3}) + \epsilon$, and then calculating the values of $x(\epsilon)$ for the extremes and center of the plate from Eq. (4). (In an Ebert mounting in which the center of the camera mirror is on the x axis, the values of $x(\epsilon)$ for the two extremes are equal.) The equations are then solved for the value of ϵ , so that $x(\epsilon, \theta_{\text{center}}) = x(\epsilon, \theta_{\text{extreme}})$.

For a Czerny-Turner spectrograph, two variations of this fourth-order correction are possible. The first possibility is to require that $x(\epsilon, \theta)$ be the same for both ends of the plate, so that the plate is perpendicular to the x axis. We thus set

$$x(\epsilon, \theta_{\text{min}}) = x(\epsilon, \theta_{\text{max}})$$

and solve for ϵ . We will refer to the position of the grating determined in this way as the corrected-flat-field position. The second possibility is to require that the ends and center of the plate all lie on a straight line. For this we set

$$2x(\epsilon, \theta_{\text{center}}) = x(\epsilon, \theta_{\text{min}}) + x(\epsilon, \theta_{\text{max}})$$

and solve for ϵ . This procedure yields a focal curve which is flatter than that obtained with either the flat-field or corrected-flat-field positions, but which is

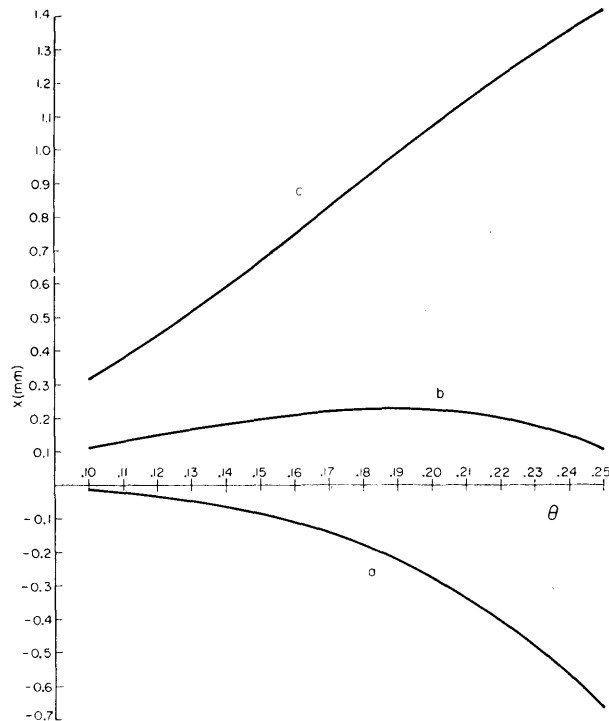


FIG. 3. Focal curves for a Czerny-Turner spectrograph with the grating at (a) flat-field position; (b) corrected-flat-field position, $\epsilon = 15$ mm; (c) super-flat-field position, $\epsilon = 39$ mm. The meaning of x and θ are given in Fig. 2.

⁸ K. Mielenz, J. Res. Natl. Bur. Std. (U. S.) 68C, 205 (1964).

slightly inclined to the y axis. We will refer to this location of the grating as the super-flat-field position.

For calculating with Eq. (4), it is useful to relate θ to β . If the grating is close to the flat-field position, then to a good approximation

$$\theta_{\min} = \sqrt{3} \beta_{\text{center}} - \sqrt{3} L/2R_2,$$

$$\theta_{\text{center}} = \sqrt{3} \beta_{\text{center}},$$

and

$$\theta_{\max} = \sqrt{3} \beta_{\text{center}} + \sqrt{3} L/2R_2,$$

where L is the length of the plate holder and β_{center} is the off-axis angle at the camera mirror for the ray from the center of the grating to the center of the plate.

To illustrate the shape of the focal curve when the grating is in the flat-field, the corrected-flat-field, and the super-flat-field positions, we have calculated the curve according to Eq. (4) for these three cases for a specific Czerny-Turner spectrograph that is currently being manufactured commercially. The focal length is 1.5 m and the plate length is 250 mm. The curves are shown in Fig. 3. It is clear that the grating should be placed in the super-flat-field position when a straight focal curve is desired. In this case, the grating is placed in the super-flat-field position by moving it 39 mm toward the camera mirror from the flat-field position.

DESIGN OF A 4-M SPECTROGRAPH

We now consider the problem of optimizing a plane-grating spectrograph having a collimating and camera mirror of 4-m focal length, a 256-mm-wide grating blazed at $63^\circ 26'$, and a 500-mm plate. This is the spectrograph discussed by Chandler.² In this analysis we follow Chandler and take the distance between the slit and plate center as 624.5 mm and the distance between the centers of the mirrors as 453.0 mm. The grating is used at angles between 55° and 70° . The grating will be placed at the super-flat-field position. The mirror separation is the minimum separation possible for the 200-mm-diam collimating and 580-mm-diam camera mirrors.⁹ The slit to plate-center distance is the minimum separation that allows the grating to be translated to the positions given by Eq. (3) without obstructing any of the light that reaches the plate.

The results obtained for this system by Chandler are summarized as follows:

(1) For the grating at an angle of about 62° , the lateral position of the grating which produces a coma-free image at the center of the plate differs by 7.5 cm from the position determined by Eq. (3). For this instrument, this implies an off-axis angle ratio $\beta/\alpha = 1.27$ compared with the ratio of 2.18 found with the \cos^3 rela-

tion. Thus, the spectrograph is much more symmetric than would have been expected according to the theory.

(2) In order to maintain satisfactory images throughout the angular region of use of a fixed grating, it is necessary to refocus the entrance slit. The total slit movement in going from 54 – 70° is 2.5 mm.

(3) The use of a fixed plate holder, either curved or flat, optimized at 62° with slit refocusing throughout the 55° to 70° region results in image widths that are much greater than the widths at best focus.

(4) A symmetric spectrograph configuration gives better images than one that satisfies the \cos^3 relation.

In order to try to confirm these conclusions, a copy of a ray-tracing program for a plane grating spectrograph was obtained from L. R. Megill. We found that in order to obtain meaningful results for this problem, the geometry had to be changed to make the x axis parallel to the entrance axis of the spectrograph.¹⁰ The geometry that we used is given in the Appendix, with several formulas that help in the calculation of the properties of the spectrograph in terms of its easily measurable dimensions.

With this change of the basic geometry, the ray-tracing program was used to calculate the image widths in the meridional plane, due to a point source at the center of the slit. The spectrograph was first optimized for a nominal angle $\theta_N = 62^\circ$. The term nominal angle is taken to mean the average of the angles of incidence and diffraction for a line at the center of the plate. When the nominal angle is zero, the direct image falls at the center of the plate. This optimization is largely an iterative procedure, which ends when the following conditions are fulfilled:

(1) The grating is located longitudinally at the super-flat-field position. Note that since the line along which this distance is measured moves when the grating is translated, the longitudinal grating position must be changed when the grating is translated.

(2) The slit is located at a distance from the collimating mirror $x = \frac{1}{2}R_1 \cos \alpha$. If the grating is not placed at this point, the grating will not be illuminated with parallel light. This will cause the position of focus at the plate to change with grating angle.

(3) The coma at the center of the plate is zero. Note that the image width is not zero, because of spherical aberration, but the irradiance distribution in the meridional plane is symmetric about the central ray.

(4) The lines are in focus over the entire plate, which has been tilted and longitudinally positioned for best over-all imaging.

¹⁰ This change was necessitated by a statement in the Megill program which sets the direction cosines of the central ray relative to the x , y , and z axes equal to -1 , 0 , and 0 , respectively. Thus, the central ray is assumed by the program to be parallel to the x axis. If the geometry is not changed, the calculated spot diagram and image width do not refer to rays which actually form the image. This is equivalent to tracing rays through a system that is different from the one specified by the input parameters.

⁹ The diameter of the camera mirror is determined by the requirement that the entire grating be visible from all points of the plate holder. This gives $D > W \cos \beta + 2L(1 - m/r)$.

In this work, the focus was determined for nine points across the plate spaced 6.25 cm apart. After we optimized the system for $\theta_N = 62^\circ$, we rotated the grating to 55° and 70° , and determined the image widths for these nine points. The grating was not translated; the slit and plate were not refocused. The results are given in Table I, in which we have given the width of the image in the meridional plane for each of the nine points across the plate, as found by the ray tracing. The coma widths as calculated from Eq. (1) have also been given. We observe that

(1) At 62° the image width is smallest where the calculated coma is zero. The image width of 0.0026 mm at this point is due to spherical aberration, which accounts for most of the image width when the coma is less than about 0.003 mm. The spherical aberration also causes the system to become slightly defocused when the grating is rotated away from 62° , owing to a change of aperture and consequent shift of the position of best focus.

(2) The image widths are in general only slightly greater than the absolute value of the calculated coma widths. The largest image width throughout the whole region of use for this fixed, flat plate with no refocusing is only 0.0205 mm. This is only slightly greater than the 0.015 mm diffraction width at 5000 Å for this $f/30$ system.

These results clearly indicate good agreement between the ray-tracing calculations and the analytic theory. In Fig. 4, the image widths given in Table I are plotted along with Chandler's results for a system with fixed

TABLE II. Image quality for a 3.34-m Czerny-Turner spectrograph with fixed slit, grating, and plate positions. System optimized for $\theta_N = 62^\circ$. Successive points across plate are separated by 6.25 cm. All entries in table are in units of 0.001 mm. The ray-tracing width is the maximum separation between rays in the meridional plane, found by ray tracing. The calculated coma is the coma width found from Eq. (1). A plus sign indicates a flare away from the slit; a minus sign indicates a flare toward the slit. Where no sign is given for the ray tracing width, the meridional rays were found to be symmetric about the central ray. The ray-tracing length (astigmatism) is the extension of the image perpendicular to the meridional plane, as found by ray tracing.

		Slit side		Center		Far side
$\theta_N = 52^\circ$	Ray-tracing width	-9.2	4.5	+9.0	+14.6	+20.0
	Calculated coma	-7.2	+0.9	+8.0	+14.0	+19.0
	Ray-tracing length (astigmatism)	122	207	327	480	668
$\theta_N = 55^\circ$	Ray-tracing width	-8.4	3.9	+6.7	+11.0	+14.7
	Calculated coma	-7.2	-0.4	+5.3	+10.0	+13.8
	Ray-tracing length (astigmatism)	117	196	309	453	630
$\theta_N = 62^\circ$	Ray-tracing width	-6.8	-3.7	2.9	+3.4	+4.0
	Calculated coma	-6.8	-3.0	-0.0	+2.1	+3.4
	Ray-tracing length (astigmatism)	102	164	264	385	534
$\theta_N = 70^\circ$	Ray-tracing width	-6.1	-5.3	-4.9	-5.5	-7.0
	Calculated coma	-5.8	-4.5	-3.9	-3.9	-4.5
	Ray-tracing length (astigmatism)	81	132	205	298	412

slit, grating, and plate positions. It can be seen that the properties of the 4-m spectrograph as given here are very different from those given by Chandler. A possible reason for this disagreement is that Chandler did not take into account the program's assumption that the central ray enters the spectrograph parallel to the x axis.

Note added in proof. In a recent letter⁷ Chandler has informed me that he did not take this aspect of the program into account. We thus agree that this explains the discrepancy between his ray tracing results and those given here.

DESIGN OF THE NBS 3.34-M SPECTROGRAPH

We have recently put into operation a photographic Czerny-Turner spectrograph for the air region, which has a 3.34-m focal length. The instrument has a collimating mirror with 254-mm diam, a camera mirror with 406-mm diam, a 220×135 -mm grating with 300 lines/mm, blazed at $63^\circ 26'$, and a 254-mm plate holder. The spectrograph was designed, according to the analytic theory, to have zero coma at the center of the plate for a nominal grating angle of 62° . Although the grating table has been mounted on an accurate cross feed to provide a translation movement if eventually desired, no translation of the grating is contemplated with the present design. The grating is used at nominal angles from 52° to 70° for complete coverage of the photographic spectrum.

The camera mirror is one that was available to us as a component of an older, surplus spectrograph. The properties of this mirror, after being refocused, fixed its radius of curvature at 6681 mm for the design calculations. The design was carried out by first placing the two mirrors as close together as possible in the z direction (see Appendix). The slit, grating, and plate were also placed as close together as possible in the z direction. In its optimum position, the grating may be rotated to a nominal angle of about 50° without interfering with light directed to the slit side of the plate. The grating was assumed to be in the super-flat-field position. With the components placed in this way, the

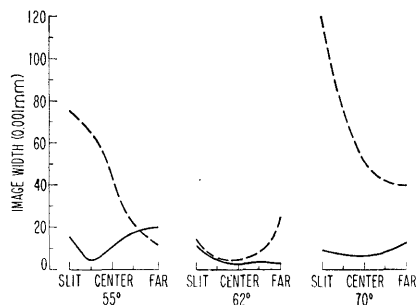


FIG. 4. Image widths for an optimized 4-m Czerny-Turner spectrograph with fixed slit, grating, and plate positions found in present work (solid line) compared with results of Chandler² (broken line).

TABLE I. Image quality for a 4-m Czerny-Turner spectrograph with fixed slit, grating, and plate positions. System optimized for $\theta_N=62^\circ$. Successive points across plate are separated by 6.25 cm. All entries in table are in units of 0.001 mm. The ray-tracing width is the maximum separation between rays in the meridional plane found by ray tracing. The calculated coma is the coma width found from Eq. (1). A plus sign indicates a flare away from the slit; a minus sign indicates a flare toward the slit. Where no sign is given for the ray tracing width, the meridional rays were found to be symmetric about the central ray. The ray-tracing length (astigmatism) is the extension of the image perpendicular to the meridional plane, as found by ray tracing.

		Slit side			Center				Far side	
$\theta_N=55^\circ$	Ray-tracing width	-15.9	-9.2	4.5	+7.2	+10.8	+14.5	+17.4	+19.3	+20.5
	Calculated coma	-13.4	-6.7	-0.8	+4.2	+8.5	+12.0	+14.7	+16.6	+17.9
	Ray-tracing length (astigmatism)	220	305	416	554	717	906	1122	1363	1630
$\theta_N=62^\circ$	Ray-tracing width	-11.6	-7.6	-5.1	-3.2	2.6	+2.8	+3.3	+3.3	+2.7
	Calculated coma	-11.3	-7.4	-4.2	-1.8	+0.0	+1.1	+1.6	+1.4	+0.6
	Ray-tracing length (astigmatism)	189	261	354	470	607	767	948	1151	1375
$\theta_N=70^\circ$	Ray-tracing width	-9.4	-8.1	-7.1	-6.7	-6.6	-7.1	-8.5	-10.4	-12.9
	Calculated coma	-8.6	-7.2	-6.3	-6.0	-6.3	-7.0	-8.3	-10.0	-12.3
	Ray-tracing length (astigmatism)	148	203	275	363	469	591	729	885	1057

radius of the collimating mirror R_1 was the only parameter that could still be varied. The value of R_1 was set by requiring that the coma calculated from Eq. 1 be zero at the center of the plate for $\theta_N=62^\circ$. Note that this entails an iterative calculation, since α , and to a lesser extent α_θ and β_θ , depend on the value of R_1 . The finally adopted parameters were: $R_1=6990$ mm; distance between centers of mirrors, $E_1=396$ mm; distance between slit and center of plate, $E_2=350$ mm; distance between entrance axis and center of grating, $z_\theta=123$ mm. Other parameters of interest are: $h=2813$ mm; $x_\theta=2954$ mm; $m=3872$ mm; $\alpha=0.0208$; $\beta_{\text{center}}=0.0418$; β_θ (center of plate) $-\alpha_\theta=7.95^\circ$.

This design results in a coma-free system at the center of the plate in the blaze with a minimum of astigmatism. (The astigmatism is proportional to the square of the off-axis angle and is additive for the two mirror reflections.) This method for simultaneously reducing both coma and astigmatism has also been used in a recent model of a 0.75-m spectrograph manufactured by Spex Industries.

In Table II we have given the calculated properties of the present design. The image width is the maximum separation of rays in the meridional plane, as given by ray tracing. In general, the calculated image widths are comparable to the diffraction width of 0.015 mm; we therefore conclude that this design produces acceptable images throughout the angular range of the grating. The lengths of the astigmatic images in this design are about half as great as the astigmatic lengths for corresponding points on the plate relative to the plate center in the 4-m design given in Table I.

An advantage of Chandler's spectrograph over the present 3.34-m instrument is its increased wavelength coverage in a single exposure, because of its larger plate. Comparison of Tables I and II shows that, when properly optimized,¹¹ this increased coverage can be achieved without much loss of image quality.

In determining the best position for the slit relative to the collimating mirror in these design calculations, the presence of spherical aberration can play a minor, but not completely negligible, role. At any grating angle, the position of best focus at the plate is determined by the location of the circle of least confusion, whose location in turn depends upon the aperture of the system. As we have already noted, when the grating rotates to different angles, the effective aperture of the system changes, and in principle the position of best focus also changes. A calculation of the extent of this effect for the present system shows a change of focal setting of about 0.15 mm, as the grating rotates through the useful angular range. Although this change of focus may not be significant, it can be completely eliminated by positioning the slit so that the change of focus caused by not having the slit at the $\frac{1}{2}R_1 \cos\alpha$ position cancels the change of focus due to the change of aperture. For the results in Table II, the slit was displaced outward from the $\frac{1}{2}R_1 \cos\alpha$ position by 0.5 mm. This made the focal setting for the center of the plate at $\theta_N=52^\circ$ the same as for $\theta_N=62^\circ$. When this is done, the images at $\theta_N=70^\circ$ are slightly out of focus, but the aperture of the system is so small at this high angle that the resultant images are still very sharp.

Displacement of the slit from the $\frac{1}{2}R_1 \cos\alpha$ position has been used by Fastie¹¹ to compensate for changes of focus due to curvature of the grating blank in actual spectrographs.

EXPERIMENTAL

A series of exposures was made to compare the coma-free grating position with the position calculated from the analytic theory. The light source was a He-Ne laser ($\lambda 6328 \text{ \AA}$). The light was first diffused by a stationary ground-glass plate and then by a rotating

¹¹ W. G. Fastie, private communication.

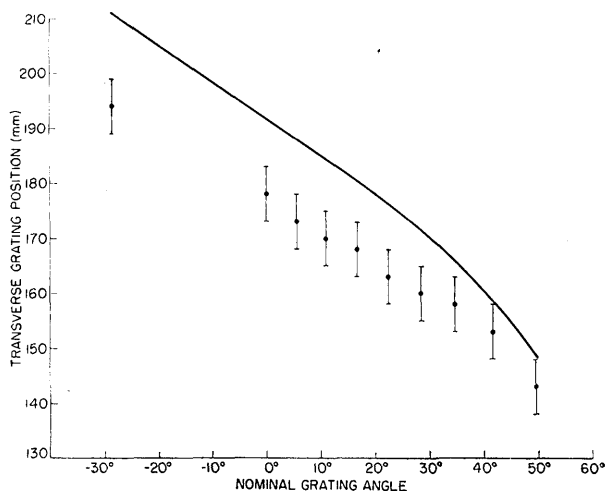


FIG. 5. Calculated and experimental transverse grating positions, z_g (see appendix), for a coma-free image at the center of the plate for the present 3.34-m Czerny-Turner spectrograph. Experimental points have error bars.

ground-glass plate. Light from the rotating plate was focused onto the spectrograph slit. This diffusion process enabled us to fill the grating with a monochromatic beam of light. The exposures were made by positioning the laser line in a particular order at the center of the plate and then taking pictures of the line at successive transverse grating positions. At each transverse position, the mirrors were rotated to follow the grating. The laser line was photographed at approximately six different focal settings of the plate for each transverse grating position. We found that the coma could be best observed in the pictures taken with the plate just inside the position of best focus. At this point, the image breaks up into two separate lines that are equal in intensity when the coma has been eliminated. This is equivalent to observing an out-of-focus lens image to determine whether the lens is properly oriented. Our efforts to observe an asymmetry in the image at best focus at the higher grating angles were frustrated by a slight asymmetry caused by the grating itself. However, at the low grating angles the asymmetry at best focus was easily observable, and the coma-free grating position determined at best focus agreed with that found with the out-of-focus method. This gave us confidence in the results of the out-of-focus method at the higher angles.

At angles higher than about 50° , the out-of-focus image became more complicated, and it was thus not possible to determine a coma-free grating position. The complications in the out-of-focus image are probably due to imperfections in the optical surfaces, which produce distortions in the wavefront comparable to the coma distortions at low apertures. Thus, the present spectrograph, having an aperture ratio of about $f/30$ in the blaze, is too slow to check the theory at high angles. From this, we conclude that at aperture ratios

of $f/30$ or greater, coma is not an important aberration for any reasonable arrangement.

The results obtained at the angles for which a coma-free grating position could be determined are given in Fig. 5. Although the observed positions generally follow the theoretical predictions, there is definitely a systematic difference which we have not yet been able to explain. Fortunately, the observations and predictions appear to be converging for angles in the actual region of use of the grating.

DISCUSSION

It should be emphasized that the results of the analytic theory and of the ray tracing given here, except for the length of the images due to astigmatism given in Tables I and II, are based on a two-dimensional treatment. As far as we know, no existing three-dimensional theory of the Czerny-Turner spectrograph is available. For the ray-tracing method, the evaluation of the full effect of the out-of-plane rays would require tracing rays from successive points along the slit to determine the curvature of the over-all slit image relative to the curvature of the individual spot diagrams. These three dimensional considerations are beyond the scope of this work. The relatively good agreement between the two-dimensional theory and the observations with the 3.34-m instrument shows that the optimum grating position will not be significantly affected by a three-dimensional treatment. It is possible though that such a treatment may explain the systematic differences seen in Fig. 5.

ACKNOWLEDGMENTS

I would like to thank Dr. L. R. Megill of the Environmental Sciences Service Administration for making the ray-tracing program available and for his help in getting the program to run on the NBS computer. The continued encouragement of Dr. W. C. Martin throughout this work is also greatly appreciated.

APPENDIX

We give here some geometrical formulas that are helpful in calculating the properties of a Czerny-Turner spectrograph in terms of its easily measurable dimensions. We have assumed that the line through the center of the plate and the slit is perpendicular to the

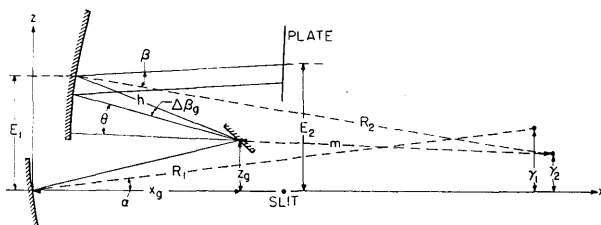


FIG. 6. General geometry of a Czerny-Turner spectrograph.

x axis. The formulas are approximate, in the sense that $\sin \varphi = \tan \varphi = \varphi$. The meaning of the symbols is given in Fig. 6.

(1) Off-axis angle at collimating mirror

$$\alpha = z_0 / 2x_0.$$

(2) Off-axis angle at camera mirror

$$\beta = (E_1 + h\Delta\beta_0 - z_0) / 2l + (E_2 + \frac{1}{2}R_2\Delta\beta_0 - E_1 - h\Delta\beta_0) / R_2,$$

where

$$\Delta\beta_0 = \beta_0 - \beta_0 \text{ (center of plate)}$$

$$l = [h^2 - (E_1 - z_0)^2]^{\frac{1}{2}}.$$

(3) z coordinates of the centers of curvature of mirrors

$$\gamma_1 = z_0 R_1 / 2x_0$$

$$\gamma_2 = E_2 - R_2(E_1 - z_0) / 2l.$$

(4) x coordinates of the points where the tangents to the mirrors are parallel to the z axis

$$\delta_1 = [R_1^2 - \gamma_1^2]^{\frac{1}{2}} - R_1$$

$$\delta_2 = x_0 - l - R_2 + [R_2^2 - (E_1 - \gamma_2)^2]^{\frac{1}{2}}.$$

(5) Distance between center of curvature of camera mirror and center of grating

$$m = \{ (l - [R_2^2 - (E_1 - \gamma_2)^2]^{\frac{1}{2}})^2 + (z_0 - \gamma_2)^2 \}^{\frac{1}{2}}.$$

(6) Plate-position parameter

$$\theta = \arcsin[(R_2/m) \sin \beta].$$

(7) Slope of plate relative to z axis

$$\text{Slope} = \frac{z_0 - \gamma_2}{[R_2^2 - (E_1 - \gamma_2)^2]^{\frac{1}{2}} - l}.$$

If the slope is positive, the far side of plate is displaced away from camera mirror.

(8) Difference between angles of incidence and diffraction at the grating, for light focused on the center of the plate

$$\beta_0 \text{ (center of plate)} - \alpha_0 = (E_1 - z_0) / l + z_0 / x_0.$$



Dr. Edward U. Condon (Ives Medalist) and Mrs. Condon at Banquet, Pittsburgh meeting.